Available online at www.sciencedirect.com
SCIENCE DIRECT®
C. R. Mecanique 333 (2005) 666–675
COMPTES RENDUS MECANIQUE
http://france.elsevier.com/direct/CRAS2B/

Computational AeroAcoustics: from acoustic sources modeling to farfield radiated noise prediction

Some useful hybrid approaches for predicting aerodynamic noise

Christophe Bailly [a], Christophe Bogey [a], Xavier Gloerfelt [b]

[a] *Laboratoire de mécanique des fluides et d'acoustique UMR CNRS 5509 & École centrale de Lyon, 36, avenue Guy de Collongue, 69134 Ecully cedex, France*

[b] *Laboratoire de simulation numérique en mécanique des fluides (SINUMEF), ENSAM, 151, boulevard de l'hôpital, 75013 Paris, France*

Available online 9 September 2005

Abstract

In recent years, several numerical studies have shown the feasibility of Direct Noise Computation (DNC) where the turbulent flow and the radiated acoustic field are obtained simultaneously by solving the compressible Navier–Stokes equations. The acoustic radiation obtained by DNC can be used as reference solution to investigate hybrid methods in which the sound field is usually calculated as a by-product of the flow field obtained by a more conventional Navier–Stokes solver. A hybrid approach is indeed of practical interest when only the non-acoustic part of the aerodynamic field is available. In this review, some acoustic analogies or hybrid approaches are revisited in the light of CAA. ***To cite this article: C. Bailly et al., C. R. Mecanique 333 (2005).***

Résumé

Utilisation de quelques méthodes hybrides pour prédire le bruit d'origine aérodynamique. Plusieurs travaux récents ont montré la faisabilité d'un calcul direct du bruit d'origine aérodynamique par résolution des équations de Navier–Stokes compressibles. Le champ acoustique obtenu par ce calcul direct peut servir de solution de référence pour étudier les méthodes hybrides, où le champ acoustique rayonné est calculé à partir d'une solution des équations de Navier–Stokes obtenue avec un solver conventionnel. Les méthodes hybrides sont en effet destinées à prévoir le champ sonore lorsqu'il est difficile d'effectuer un calcul aérodynamique compressible. Dans cet article, quelques analogies acoustiques sont revisitées en s'appuyant sur des résultats de l'aéroacoustique numérique. ***Pour citer cet article : C. Bailly et al., C. R. Mecanique 333 (2005).***

Keywords: Acoustics; Computational acoustics; Lighthill's analogy; Ffowcs Williams and Hawkings analogy; Propagation in flows; Diffraction

Mots-clés : Acoustique ; Aéroacoustique numérique ; Analogie de Lighthill ; Analogie de Ffowcs Williams et Hawkings ; Propagation en écoulement ; Diffraction

* Corresponding author.
E-mail address: christophe.bailly@ec-lyon.fr (C. Bailly).
URL: http://acoustique.ec-lyon.fr.

1631-0721/$ – see front matter
doi:10.1016/j.crme.2005.07.006

1. Introduction

Methods for predicting aerodynamic noise were mainly semi-empirical in the past, and were based on the power laws established by Lighthill [1] and by others later. Over the last ten years, advances in Computational Fluid Dynamics (CFD), and especially unsteady calculations, have made accurate predictions possible. Engineering methods take advantage of this progress to improve predictions by substituting flow parameters of semi-empirical models by computed values.

The most spectacular feature of this period has been the rapid development of Computational AeroAcoustics (CAA). Two types of methods have been considered in CAA. In the first, concepts that appeared early in aeroacoustics, namely acoustic analogies or hybrid approaches, are applied using time-dependent CFD data. In the second, the aerodynamic field and the acoustic field are both calculated by solving the compressible unsteady Navier–Stokes equations. This Direct Noise Computation (DNC) is ambitious, and allows for a more physical investigation of noise source mechanisms, but serious numerical issues must be first addressed. The goals of the two classes of methods are different, but in the end, the aeroacoustics community needs both groups of predictive methods to face practical applications.

In the present paper, some acoustic analogies or hybrid approaches are revisited in the light of CAA results. Two topics are especially tackled. The first is concerned with the interpretation of the linear and non-linear parts of Lighthill's source term. The discussion is illustrated with the noise generated by vortex pairings in a forced mixing layer. This test case has the advantage of having a localized aerodynamic source with mean flow effects on the radiated noise. It is also not numerically expensive. Furthermore a reference solution based on DNC is also available [2]. The second topic deals with the presence of solid surfaces. A recent application dealing with flow-induced cylinder noise is considered [3].

2. Lighthill's analogy

2.1. Formulation

The first formulation of an acoustic analogy was derived by Lighthill [1] in 1952. The compressible fluid dynamic equations are recast into an inhomogeneous wave equation, which yields:

$$\Box\rho(\mathbf{x},t) \equiv \left(\frac{\partial^2}{\partial t^2} - c_\infty^2\nabla^2\right)\rho(\mathbf{x},t) = \frac{\partial^2 T_{ij}}{\partial x_i \partial x_j} \tag{1}$$

where $\Box$ is the D'Alembertian operator, and $T_{ij} = \rho u_i u_j + (p - c_\infty^2\rho)\delta_{ij} + \tau_{ij}$ represents a distribution of equivalent noise sources. Here, ρ, u_i, p and τ_{ij} are the instantaneous density, velocity components, pressure and viscous stress tensor. The subscript ∞ denotes the state of fluid at rest in the far field and c_∞ is the speed of sound. To simplify the discussion, the contribution of viscous terms and entropy fluctuations are assumed to be negligible and Lighthill's tensor is reduced to $T_{ij} \simeq \rho u_i u_j$. These assumptions could be relaxed if necessary. For an observer far from the source volume occupied by the turbulent velocity field, the acoustical density fluctuations in 3D free space are given by:

$$\rho'(\mathbf{x},t) \simeq \frac{1}{4\pi c_\infty^4 x}\frac{x_i x_j}{x^2}\int \frac{\partial^2 T_{ij}}{\partial t^2}\left(\mathbf{y}, t - \frac{|\mathbf{x}-\mathbf{y}|}{c_\infty}\right)\mathrm{d}\mathbf{y} \tag{2}$$

where $\rho'(\mathbf{x},t) = \rho(\mathbf{x},t) - \rho_\infty$, $\mathbf{x}$ is the observer position and $\mathbf{y}$ the source position. Many other integral formulations can be derived from (1), and a review on these subtle integral formulations can be found in Crighton [4]. The classical interpretation of Eq. (2) is given in Fig. 1.

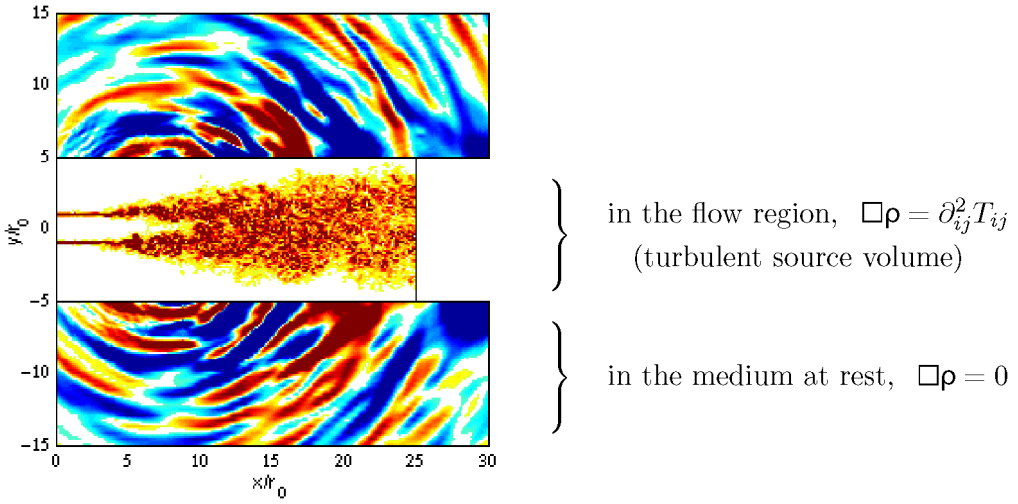

Fig. 1. Interpretation of Lighthill's analogy. As an illustration, a snapshot of the DNC of subsonic jet noise is shown with the vorticity field in the flow and the radiated acoustic pressure outside, from Bogey and Bailly [5]. A hypothetical apparatus measuring the D'Alembertian $\Box\rho$ will see a mathematical source term $\partial_{ij}^2 T_{ij}$ in the flow region, and will measure zero outside.

Fig. 1. Interprétation de l'analogie de Lighthill. L'image représente le résultat d'un calcul direct du bruit d'un jet subsonique avec le champ de vorticité dans l'écoulement et le champ de pression rayonné à l'extérieur, d'après Bogey et Bailly [5]. En imaginant posséder un D'Alembertomètre mesurant $\Box\rho$, celui-ci indiquerait le terme source mathématique $\partial_{ij}^2 T_{ij}$ dans l'écoulement, et zéro à l'extérieur.

2.2. Numerical implementation

For a numerical implementation of Lighthill's analogy, as it is shown by Sarkar and Hussaini [6] or Bastin et al. [7], the temporal formulation (2) is more appropriate and more accurate than the formulations based on the spatial derivatives of T_{ij}. The retarded-time problem is often replaced by a time accumulation method for the observer [6] in which the source time becomes the reference time and the observer time is imposed by $t + |\mathbf{x} - \mathbf{y}|/c_\infty$. Note that it is hazardous to merely approximate the source term at the retarded time by its closest value available in the computation. For two-dimensional problems, the computation of the integral solution of (1) in the Fourier space is recommended since the convolution with the 2D Green function has an infinite time integral [8,9].

The necessary truncation of the source volume in numerical simulations is also a serious difficulty. This problem was first discussed with the numerical estimation of the noise of a bounded isotropic homogeneous turbulence by Witkowska and Juvé [10]. The most common case is, however, encountered when the turbulent flow crosses the outflow boundary of the integration volume. Indeed, velocity fluctuations should vanish on the boundaries of the considered source volume in (2) but they do not and a radiation more efficient than the physical one is present in the computed solution. Ad hoc methods have been proposed as in [11,12] for instance, or by tapering the source term on the boundaries by a decreasing Gaussian function [2,7].

Another way to obtain the correct solution is to consider the Ffowcs Williams and Hawkings (FWH) formulation [13] but the calculation must be in general compressible since the fluctuating pressure, including acoustics, is required on the surface enclosing the control volume. A very simple illustration of the FWH formulation has been recently proposed by Casper et al. [14] with the case of a Taylor vortex convected in a uniform flow. The FWH formulation is presented in Section 5.

2.3. Mean flow effects

The case of a turbulent flow surrounded by a uniform mean flow, shown in Fig. 2, is now considered in order to illustrate the inclusion of mean flow – acoustics interaction in Lighthill's tensor. The acoustic fluctuations are governed by the convected wave equation:

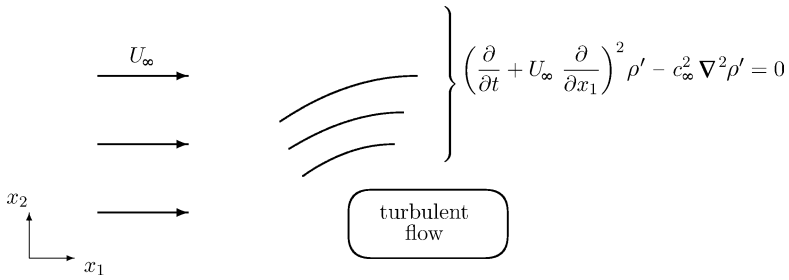

Fig. 2. Sketch of a bounded turbulent source volume generating noise in a uniform mean flow.

Fig. 2. Représentation d'un volume source fini émettant du bruit dans un écoulement uniforme.

$$\underbrace{\left(\frac{\partial}{\partial t} + U_\infty \frac{\partial}{\partial x_1}\rho'\right)^2}_{\text{(a)}} - c_\infty^2 \nabla^2 \rho' = 0 \tag{3}$$

To interpret Lighthill's equation in this case, we introduce the decomposition of the density and velocity into Lighthill's tensor:

$$T_{ij} = \rho u_i u_j = \left(\rho_\infty + \rho'\right)\left(U_\infty \delta_{1i} + u_i'\right)\left(U_\infty \delta_{1j} + u_j'\right)$$

a straightforward calculation then yields the following expression from Eq. (1):

$$\underbrace{\frac{\partial^2 \rho'}{\partial t^2}}_{\text{(b)}} - c_\infty^2 \nabla^2 \rho' = \frac{\partial^2}{\partial x_i \partial x_j}\left(\rho u_i' u_j'\right) \underbrace{-2U_\infty \frac{\partial^2 \rho'}{\partial t \partial x_1} - U_\infty^2 \frac{\partial^2 \rho'}{\partial x_1^2}}_{\text{(c)}} \tag{4}$$

By noting from (3) and (4) that (a) = (b) + (c), the linear part (c) of T_{ij} is shown to be a propagation term corresponding to mean-flow effects on acoustics. For practical applications, we often intend to get an estimate of the radiated noise from an incompressible turbulent computation which is less expensive. However by using only the incompressible part of the flow to construct Lighthill's tensor, the acoustic-mean flow interactions are lost and sound waves propagate without being affected by the presence of the mean flow.

In a more general case than the one of Fig. 2, the following splitting of the velocity $u_i = \bar{u}_i + u_i'$ is introduced into Lighthill's tensor:

$$T_{ij} = \underbrace{\rho u_i' u_j'}_{T_{ij}^f} + \underbrace{\rho \bar{u}_i u_j' + \rho u_i' \bar{u}_j + \rho \bar{u}_i \bar{u}_j}_{T_{ij}^l} \tag{5}$$

The first part T_{ij}^f involves quadratic velocity fluctuations, and is responsible for the self-noise component in (2). The second part T_{ij}^l is linear in fluctuations, and the contribution of the two first terms to (2) is called the shear-noise according to Lilley [15]. This decomposition into quadratic and linear terms is well known in the field of incompressible turbulence where the fluctuating pressure generated by a velocity field satisfies the Poisson equation:

$$-\frac{1}{\rho_\infty}\nabla^2 p' = \frac{\partial^2}{\partial x_i \partial x_j}\left(u_i' u_j' - \overline{u_i' u_j'}\right) + 2\frac{\partial \bar{u}_i}{\partial x_j}\frac{\partial u_j'}{\partial x_i} \tag{6}$$

The first source term in (6) is associated to the slow part of pressure while the term involving the mean velocity gradients is associated to the rapid part, which is the leading term in the rapid distortion theory. This starting

equation was used for instance by Kraichnan [16] to derive a statistical modelling of pressure fluctuations in a turbulent boundary layer.

Reverting to the compressible case, as pointed out by Pridmore-Brown [17] and Lilley [18] among others, the linear terms in (5) are also propagation terms. Assuming a sheared mean flow $\bar{u}_i = \overline{U}_1(x_2)\delta_{1i}$ the following inhomogeneous wave equation can be written:

$$\frac{\bar{D}}{\bar{D}t}\left(\frac{1}{c_\infty^2}\frac{\bar{D}^2 p}{\bar{D}t^2} - \nabla^2 p\right) + \underbrace{2\frac{d\overline{U}_1}{dx_2}\frac{\partial^2 p}{\partial x_1 \partial x_2}}_{\text{(f)}} = \underbrace{\frac{\bar{D}}{\bar{D}t}\frac{\partial^2 \rho u_i' u_j'}{\partial x_i \partial x_j}}_{\text{(d)}} - \underbrace{2\frac{d\overline{U}_1}{dx_2}\frac{\partial^2 \rho u_2' u_j'}{\partial x_1 \partial x_j}}_{\text{(e)}} \tag{7}$$

It is now a third order differential equation where $\bar{D}/\bar{D}t$ denotes the material derivative along the mean flow. The wave operator appearing on the left-hand side of (7) is identical to that derived from the linearized Euler equations. As a result, all the mean flow – acoustic interactions are included in this propagation operator for a sheared mean flow. The two source terms (d) and (e) on the right-hand side are now quadratic in velocity fluctuations. The term (d) comes directly from the non-linear term T_{ij}^f in Lighthill's equation (5). The term (e) from the splitting of the shear-noise term T_{ij}^l of Eq. (5) into a propagation term (f) and the source term (e).

Using the analogy defined by Eq. (7), the source term can be constructed from an incompressible time-dependent Navier–Stokes solution and mean flow effects are now provided by the wave operator. However, the homogeneous solution of (7) is known as the compressible generalization of Rayleigh's equation and instability waves are also solution of the problem. This point is discussed in [20].

3. Other hybrid methods

At least two groups of acoustic analogies have been developed since the Lighthill theory of noise. In the first one, reformulations of Lighthill's equation were proposed to emphasize the role of vorticity in the production of sound. The source term is expressed through the Lamb vector $\mathbf{L} = \boldsymbol{\omega} \times \mathbf{u}$ by noting that:

$$\nabla \cdot \nabla \cdot (\mathbf{uu}) = \nabla \cdot (\boldsymbol{\omega} \times \mathbf{u}) + \nabla^2\left(\frac{\mathbf{u}^2}{2}\right)$$

and one of the first formulations of the vortex sound theory was proposed by Powell [19] for low Mach number flows:

$$\frac{\partial^2 \rho}{\partial t^2} - c_\infty^2 \nabla^2 \rho \simeq \rho_\infty \nabla \cdot (\boldsymbol{\omega} \times \mathbf{u})$$

Vorticity-based formulations are very useful for analytical studies, but they are usually not recommended for numerical simulations [4].

The second group of methods corresponds to hybrid methods based on a wave operator including all mean flow effects to remove the linear part of Lighthill's tensor from the source term. In particular, a reformulation of Eq. (7) based on Linearized Euler's Equations (LEE) can be derived, see [20] for details and comments:

$$\begin{cases} \dfrac{\partial \rho'}{\partial t} + \nabla \cdot (\rho' \bar{\mathbf{u}} + \bar{\rho}\mathbf{u}') = 0 \\ \dfrac{\partial (\bar{\rho}\mathbf{u}')}{\partial t} + \nabla \cdot (\bar{\rho}\bar{\mathbf{u}}\mathbf{u}') + \nabla p' + (\bar{\rho}\mathbf{u}' + \rho'\bar{\mathbf{u}}) \cdot \nabla \bar{\mathbf{u}} = \mathbf{s} \qquad s_i = -\bar{\rho}\dfrac{\partial u_i' u_j'}{\partial x_j} \\ \dfrac{\partial p'}{\partial t} + \nabla \cdot [p'\bar{\mathbf{u}} + \gamma \bar{p}\mathbf{u}'] + (\gamma - 1)p'\nabla \cdot \bar{\mathbf{u}} - (\gamma - 1)\mathbf{u}' \cdot \nabla \bar{p} = 0 \end{cases} \tag{8}$$

4. Application to the noise generated by a forced mixing layer

For aerodynamic noise, the sound generated by a plane mixing layer is a very useful model problem. The flow parameters are given in Fig. 3. A direct computation of the generated noise was performed by Bogey et al. [2] to obtain the aerodynamic field and a portion of the acoustic field. The flow development is driven by forcing the mixing layer at discrete frequencies so that only the sound generated by the first vortex pairing is observed in the computational domain. This vortex pairing occurs at $x \simeq 70\delta_\omega(0)$ and the wavelength of the radiated field is $\lambda \simeq 51\delta_\omega(0)$ where $\delta_\omega(0)$ is the initial vorticity thickness.

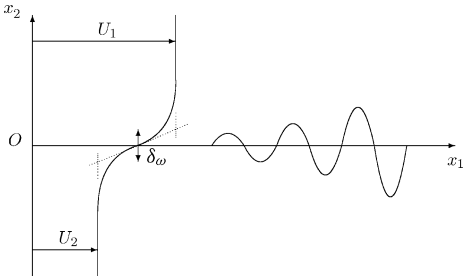

Fig. 3. Sketch of the mean flow formed by two isothermal streams at Mach $M_1 = 0.12$ and $M_2 = 0.48$ in the lower and upper parts, respectively. The mean velocity profile is given by $\bar{u}_1(x_2) = u_m[1 + R_u \tanh(2x_2/\delta_\omega)]$ with $u_m = (U_1 + U_2)/2 = 100\ \mathrm{m\,s^{-1}}$ and $R_u = (U_1 - U_2)/(2u_m) = 0.6$. $Re_\omega = \delta_{\omega(0)}(U_1 - U_2)/\nu = 12\,800$ where $\delta_{\omega(0)}$ is the initial vorticity thickness.

Fig. 3. Croquis de la couche de mélange formée par deux écoulements isothermes de nombre de Mach $M_1 = 0{,}12$ et $M_2 = 0{,}48$ en haut et en bas respectivement. Le profil de la vitesse moyenne est donné par $\bar{u}_1(x_2) = u_m[1 + R_u \tanh(2x_2/\delta_\omega)]$ avec $u_m = (U_1 + U_2)/2 = 100\ \mathrm{m\,s^{-1}}$ et $R_u = (U_1 - U_2)/(2u_m) = 0{,}6$. $Re_\omega = \delta_{\omega(0)}(U_1 - U_2)/\nu = 12\,800$ où $\delta_{\omega(0)}$ est l'épaisseur de vorticité initiale.

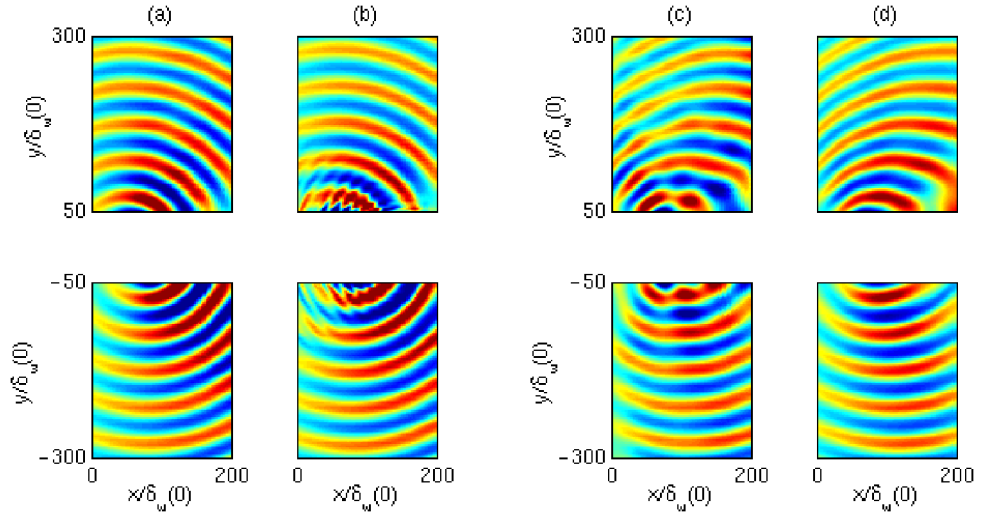

Fig. 4. Noise generated by a mixing layer. Dilatation fields obtained: from Lighthill's integral with (a) T_{ij}^f and (c) T_{ij} as source terms, (b) from the LEE without mean flow, (d) by direct noise calculation (reference solution). All the calculations are two-dimensional, and quantitative comparisons can be found in [21,22].

Fig. 4. Bruit produit par une couche de mélange. Champs de la dilatation obtenus : avec l'intégrale de Lighthill en utilisant (a) T_{ij}^f et (c) T_{ij}, (b) avec les équations d'Euler linéarisées sans écoulement moyen, (d) par calcul direct du bruit (solution de référence). Tous les calculs sont bidimensionnels et des comparaisons quantitatives sont dans [21,22].

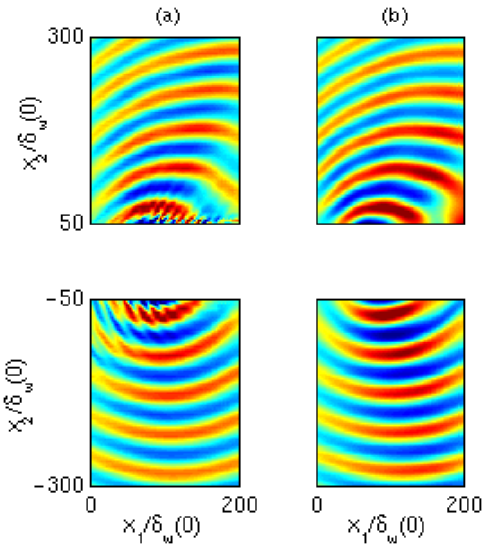

Fig. 5. Dilatation fields obtained: (a) from the LEE (8), (b) by direct noise calculation (reference solution).

Fig. 5. Champ de dilatations obtenus : (a) avec les équations d'Euler linéarisées (8), (b) par calcul direct du bruit (solution de référence).

Fig. 4(d) shows a snapshot of the dilatation field $\Theta = \nabla \cdot \mathbf{u}$, which is directly linked to the fluctuating pressure field in the present case [21]. Mean flow effects on propagation are well marked especially in the rapid stream region. The acoustic field predicted by Lighthill's analogy with the quadratic term $T_{ij}^f = \rho u_i' u_j'$ only is shown in Fig. 4(a) whereas the acoustic field predicted by Lighthill's theory with the full tensor T_{ij} is displayed in Fig. 4(c). This source term T_{ij} including all interactions between the flow and the acoustic waves, the solution 4(c) is in agreement with the direct computation of noise in 4(d). Note finally that Fig. 4(a) compares with Fig. 4(b) corresponding to the solution obtained by LEE (8) without mean flow effects ($\bar{\mathbf{u}} = 0$), that Lighthill's solutions were obtained with the 2D Green function for consistent comparisons [22] and that the integrations are performed over the whole domain defined by $0 \leqslant x_1 \leqslant 200\delta_\omega(0)$ and $-300\delta_\omega(0) \leqslant x_2 \leqslant 300\delta_\omega(0)$.

Fig. 5 shows the reference solution in (b) and the solution obtained by solving LEE (8) with the self-noise source term in (a). The two solutions are in good agreement. Finally, there are two ways to obtain the correct acoustic radiation. In the first one, illustrated by Fig. 4(c), the Lighthill tensor is constructed from a compressible solution of the Navier–Stokes solution. This problem is academic since the evaluation of the linear part of T_{ij} requires the calculation of the acoustic field, namely the solution of the problem is already known. In the second one, shown in Fig. 5(a), mean flow effects are taken into account by the wave operator and the source term $\mathbf{s}$ in (8) can be computed from an incompressible turbulent flow.

5. Influence of solid boundaries

Lighthill's theory was generalized by Ffowcs Williams and Hawkings [13] to include the presence of surfaces. A closed surface Σ is defined by $f(\mathbf{x}, t) = 0$, with $f < 0$ in the interior, $f > 0$ outside, and such that $\nabla f = \mathbf{n}$ where $\mathbf{n}$ is the outward unit normal vector. As shown in Fig. 6, the function f defines the control surface outside of which the solution is required, but a solution valid for all space is sought to derive integral formulations involving the free space Green function G. Thus, variables have the values of the undisturbed medium ρ_∞, p_∞ inside Σ and generalized functions are now considered to take into account the discontinuity across Σ thanks to jump terms.

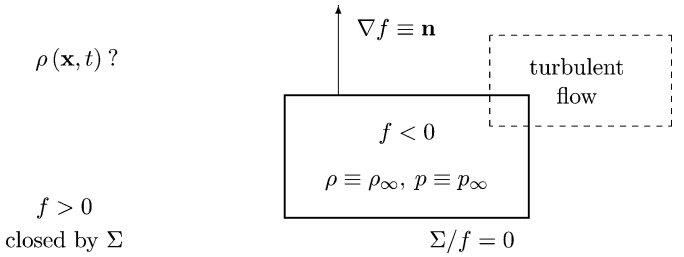

Fig. 6. Notations for the Ffowcs Williams and Hawkings formulation.

Fig. 6. Notations pour la formulation de Ffowcs Williams et Hawkings.

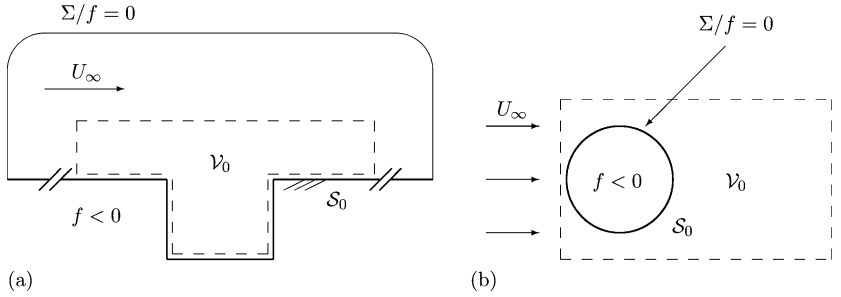

Fig. 7. Two examples of configuration for applying the Ffowcs Williams and Hawkings formulation: (a) flow past a cavity and (b) cylinder flow.

Fig. 7. Deux exemples de configuration pour appliquer la formulation de Ffowcs Williams et Hawkings : (a) écoulement au dessus d'une cavité et (b) écoulement autour d'un cylindre.

Noting H the Heaviside function and $\delta = \mathrm{H}'$ the Dirac delta function, the equation for the generalized variable $\mathrm{H}\rho' = \mathrm{H}(f)(\rho - \rho_\infty)$ [23] becomes:

$$\left(\frac{\partial^2}{\partial t^2} - c_\infty^2 \nabla^2\right)[\mathrm{H}\rho'] = \frac{\partial^2[H(f)T_{ij}]}{\partial x_i \partial x_j} + \frac{\partial[F_i \delta(f)]}{\partial x_i} + \frac{\partial[Q\delta(f)]}{\partial t} \tag{9}$$

with:

$$F_i = -\big[\rho u_i(u_j - u_j^\Sigma) + p\delta_{ij} - \tau_{ij}\big]n_j, \qquad Q = \big[\rho(u_j - u_j^\Sigma) + \rho_\infty u_j^\Sigma\big]n_j$$

and $\mathbf{u}^\Sigma$ the surface velocity. Two additional contributions of dipole and monopole type must now be evaluated on the surface Σ. Note that Lighthill's analogy (1) is recovered if the volume inside Σ vanishes, and that the turbulent flow can cross the control surface. Eq. (9) is the starting point of many developments, especially for helicopter noise predictions [24,25] or for derivating wave extrapolation methods through porous or permeable surfaces.

To simplify algebra as in the first section, the control surface is now assumed to be a stationary solid wall, which reduces (9) to Curle's equation [26], and viscous effects are disregarded. As a result, $F_i = -pn_i$ and $Q \equiv 0$. Fig. 7(a) shows for instance the configuration used to investigate the noise radiated by a grazing flow over a cavity by Gloerfelt et al. [9]. The integral surface is taken along the cavity walls $\mathcal{S}_0$ and the volume integral over the volume $\mathcal{V}_0$. All the remarks made in the first section about the interpretation of the linear part of Lighthill's tensor and about numerics, still hold. In the case of Fig. 7(a), a convected Ffowcs Williams and Hawkings equation can be derived when the observer is located in a uniform mean flow [8,9] rather than accounting for mean flow effects by integrating over the full outside volume $f > 0$ in including compressible effects in T_{ij}.

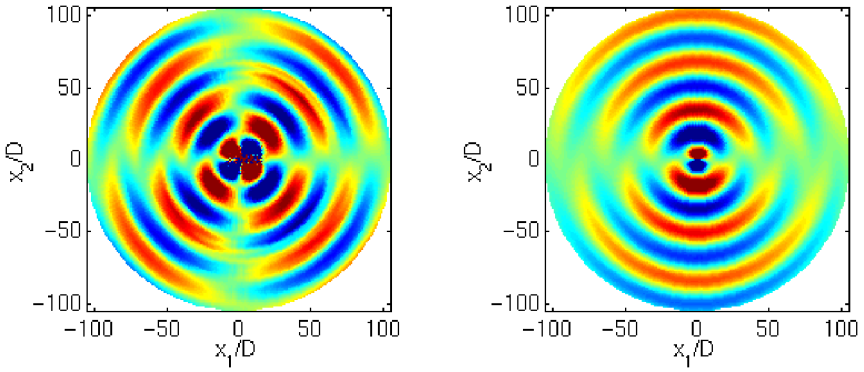

Fig. 8. Noise generated by a flow at $M_\infty = 0.12$ around a cylinder, from [3]. Eq. (10) with: on the left, contribution of the volume integral, levels of pressure ±0.5 Pa, on the right, contribution of the surface integral, levels of pressure ±5 Pa.

Fig. 8. Bruit produit par un écoulement à $M_\infty = 0,12$ autour d'un cylindre, tiré de [3]. Éq. (10) avec : à gauche, contribution de l'intégrale de volume, niveaux de pression ±0,5 Pa, à droite, contribution de l'intégrale de surface, niveaux de pression ±5 Pa.

As for Lighthill's source term, the surface integral can be calculated with a compressible or an incompressible pressure provided by Navier–Stokes solvers. Since Eq. (9) is satisfied throughout the whole space, the integral solution can take the following form:

$$\rho' = \frac{\partial^2 [H(f)T_{ij}]}{\partial x_i \partial x_j} * G - \frac{\partial [p\delta(f)]}{\partial n} * G = H(f)T_{ij} * \frac{\partial^2 G}{\partial x_i \partial x_j} - p\delta(f) * \frac{\partial G}{\partial n} \tag{10}$$

where $\partial_n = n_i \partial_i$. The second formulation is often more appropriate numerically, in particular for 2D computations in Fourier space [8,9]. Fig. 7(b) shows a sketch of the geometry for computing the æolian tone generated by a flow around a cylinder. The noise can be calculated with Eq. (10) and is well approximated by the surface integral contribution alone for low Mach number flows $M_\infty = U_\infty / c_\infty$, as shown in Fig. 8 for the cylinder case [3]. A tailored Green function $\mathcal{G}$ satisfying the boundary condition $\partial_n \mathcal{G} = 0$ on Σ can also be introduced to solve Eq. (9). The solution is then given by:

$$\rho' = \frac{\partial^2}{\partial x_i \partial x_j} \big[H(f)T_{ij} * \mathcal{G} \big]$$

which allows one to interpret the surface integral contribution of Eq. (10) as the diffraction of the turbulent sources by the cylinder itself [3,23]. The tailored Green function $\mathcal{G}$ is in general difficult to determine, at least analytically, and formulation (10) is preferred. However, the use of an incompressible solver to calculate the pressure on the surface is only valid for the low frequency limit, when the diffraction problem is governed by a Poisson equation, i.e. $\Box \to c_\infty^2 \nabla^2$ without specular acoustic reflection.

6. Concluding remarks

For low Mach number flows and complex geometries, acoustic analogies based on an incompressible Navier–Stokes solver remain a good strategy to compute radiated noise. Indeed, mean flow effects are expected to be weak and the direct computation of noise is still difficult to apply to complex configurations. Nevertheless, when strong coupling between acoustic waves and turbulence occurs or when the high-frequency component of spectra must be computed, a compressible simulation is then necessary to apply the Ffowcs Williams and Hawkings formulation, for instance.

Acknowledgements

We express our gratitude to Electricité de France for its financial support under the supervision of Dr. Philippe Lafon, and to Olivier Marsden for editorial helps.

References

[1] M.J. Lighthill, On sound generated aerodynamically. I. General theory, Proc. Roy. Soc. London 211 (A1107) (1952) 564–587.
[2] C. Bogey, C. Bailly, D. Juvé, Numerical simulation of the sound generated by vortex pairing in a mixing layer, AIAA J. 38 (12) (2000) 2210–2218.
[3] X. Gloerfelt, F. Pérot, C. Bailly, D. Juvé, Flow-induced cylinder noise formulated as a diffraction problem for low Mach numbers, J. Sound Vib. 287 (2005) 129–151.
[4] D. Crighton, Basic principles of aerodynamic noise generation, Progress Aerosp. Sci. 16 (1) (1975) 31–96.
[5] C. Bogey, C. Bailly, Investigation of subsonic jet noise using LES: Mach and Reynolds number effects, in: 10th AIAA/CEAS Aeroacoustics Conference, AIAA Paper 2004-2023 (2004).
[6] S. Sarkar, M.Y. Hussaini, Computation of the acoustic radiation from bounded homogeneous flows, in: J.C. Hardin, M.Y. Hussaini (Eds.), Computational Aeroacoustics, Springer-Verlag, 1993, pp. 335–349.
[7] F. Bastin, P. Lafon, S. Candel, Computation of jet mixing noise due to coherent structures: the plane jet case, J. Fluid Mech. 335 (1997) 261–304.
[8] D.P. Lockard, An efficient, two-dimensional implementation of the Ffowcs Williams and Hawkings equation, J. Sound Vib. 229 (4) (2000) 897–911.
[9] X. Gloerfelt, C. Bailly, D. Juvé, Direct computation of the noise radiated by a subsonic cavity flow and application of integral methods, J. Sound Vib. 266 (1) (2003) 119–146.
[10] A. Witkowska, D. Juvé, Numerical estimation of noise generated by homogeneous and isotropic turbulence, C. R. Acad. Sci. Paris, Sér. II 318 (1994) 597–602 (in French).
[11] M. Wang, S.K. Lele, P. Moin, Computation of quadrupole noise using acoustic analogy, AIAA J. 34 (11) (1996) 2247–2254.
[12] B.E. Mitchell, S.K. Lele, P. Moin, Direct computation of the sound generated by vortex pairing in an axisymmetric jet, J. Fluid Mech. 383 (1999) 113–142.
[13] J.E. Ffowcs Williams, D.L. Hawkings, Sound generation by turbulence and surfaces in arbitrary motion, Philos. Trans. Roy. Soc. London 264 (A1151) (1969) 321–342.
[14] J.H. Casper, D.P. Lockard, M.R. Khorrami, C.L. Streett, Investigation of volumetric sources in airframe noise simulation, in: 10th AIAA/CEAS Aeroacoustics Conference, AIAA Paper 2004-2805 (2004).
[15] G.M. Lilley, On the noise from air jets, British Aeronautical Research Council, A.R.C. 20-276, 1958.
[16] R.H. Kraichnan, Pressure field within homogeneous anisotropic turbulence, J. Acoust. Soc. Am. 28 (1) (1956) 64–72.
[17] D.C. Pridmore-Brown, Sound propagation in a fluid flowing through an attenuating duct, J. Fluid Mech. 4 (1958) 393–406.
[18] G.M. Lilley, The generation and radiation of supersonic jet noise. Vol. IV. Theory of turbulence generated jet noise, noise radiation from upstream sources, and combustion noise. Part II: Generation of sound in a mixing region, Air Force Aero Propulsion Laboratory, AFAPL-TR-72-53, vol. 4, 1972.
[19] A. Powell, Theory of vortex sound, J. Acoust. Soc. Am. 16 (1964) 177–195.
[20] C. Bailly, C. Bogey, Contributions of CAA to jet noise research and prediction, Internat. J. Comput. Fluid Dynam. 18 (6) (2004) 481–491.
[21] C. Bogey, C. Bailly, D. Juvé, Computation of flow noise using source terms in linearized Euler's equations, AIAA J. 40 (2) (2002) 235–243.
[22] C. Bogey, X. Gloerfelt, C. Bailly, An illustration of the inclusion of sound-flow interactions in Lighthill's equation, AIAA J. 41 (8) (2003) 1604–1608.
[23] D.G. Crighton, A.P. Dowling, J.E. Ffowcs Williams, M. Heckl, F.G. Leppington, Modern Methods in Analytical Acoustics, Springer-Verlag, London, 1992.
[24] K.S. Brentner, F. Farassat, Modeling aerodynamically generated sound of helicopter rotors, Progress Aerosp. Sci. 39 (2003) 83–120.
[25] J. Prieur, G. Rahier, Aeroacoustic integral methods, formulation and efficient numerical implementation, Aerosp. Sci. Technol. 5 (2001) 457–468; see also addendum in vol. 6, p. 323.
[26] N. Curle, The influence of solid boundaries on aerodynamic sound, Proc. Roy. Soc. London 231 (A1187) (1955) 505–514.